

Article

Hybrid Electrolyte Based on PEO and Ionic Liquid with In Situ Produced and Dispersed Silica for Sustainable Solid-State Battery

Tatiana Babkova ¹, Rudolf Kiefer ² and Quoc Bao Le ^{2,*}

¹ Centre of Polymer Systems, Tomas Bata University in Zlin, 760 01 Zlin, Czech Republic; tatianababkova@seznam.cz

² Conducting Polymers in Composites and Applications Research Group, Faculty of Applied Sciences, Ton Duc Thang University, Ho Chi Minh City 700000, Vietnam; rudolf.kiefer@tdtu.edu.vn

* Correspondence: lequocbao@tdtu.edu.vn

Abstract: This work introduces the synthesis of hybrid polymer electrolytes based on polyethylene oxide (PEO) and electrolyte solution bis(trifluoromethane)sulfonimide lithium salt/ionic liquid 1-ethyl-3-methyl-imidazolium bis(trifluoromethylsulfonyl)imide (LiTFSI/EMIMTFSI) with in situ produced and dispersed silica particles by the sol–gel method. Conventional preparation of solid polymer electrolytes was followed by desolvation of lithium salt in a polymer matrix of PEO, which, in some cases, additionally contains plasticizers. This one-pot synthesis is an alternative route for fabricating a solid polymer electrolyte for solid-state batteries. The presence of TFSI- reduces the crystallinity of the PEO matrix (plasticizing effect), increases the dissociation and solubility of LiTFSI in the PEO matrix because of a highly delocalized charge distribution, and reveals excellent thermal, chemical, and electrochemical stability. Tetraethylorthosilicate (TEOS) was chosen due to the slow reaction rate, with the addition of (3-glycidioxypropyl)trimethoxysilane (GLYMO), which contributes to the formation of a silica network. FTIR studies confirmed the interactions between the silica, the polymer salt, and EMIMTFSI. Impedance spectroscopy measurements were performed in a wide range of temperatures from 25 to 70 °C. The electrochemical performance was explored by assembling electrolytes in LiCoO₂ (LCO), NMC(811), and LiFePO₄ (LFP) coin half-cells. The HPEf15 shows a discharge capacity of 143 mA/g for NMC(811) at 0.1 C, 134 mA/g for LCO, and 139 mA/g for LFP half-cells at 0.1 C and 55 °C. The LFP half-cell with a discharge capacity of 135 mA/g at 0.1 C (safety potential range of 2.8 to 3.8) obtained a cyclability of 97.5% at 55 °C after 100 cycles. Such a type of electrolyte with high safety and good electrochemical performance provides a potential approach for developing a safer lithium-ion battery.

Keywords: PEO; ionic liquids; incorporated silica; hybrid electrolyte; energy storage



check for updates

Citation: Babkova, T.; Kiefer, R.; Le, Q.B. Hybrid Electrolyte Based on PEO and Ionic Liquid with In Situ Produced and Dispersed Silica for Sustainable Solid-State Battery. *Sustainability* **2024**, *16*, 1683. <https://doi.org/10.3390/su16041683>

Academic Editor: Zhibin Ye

Received: 23 January 2024

Revised: 13 February 2024

Accepted: 17 February 2024

Published: 19 February 2024



Copyright: © 2024 by the authors. Licensee MDPI, Basel, Switzerland. This article is an open access article distributed under the terms and conditions of the Creative Commons Attribution (CC BY) license (<https://creativecommons.org/licenses/by/4.0/>).

1. Introduction

Because of the increasing need for power, worries about global warming, and difficulties in oil supply, there has been a boom in the demand for sustainable energy sources such as batteries, solar, and wind energy in recent years. Among them, batteries are exceptionally alluring and are essential for powering electric cars and mobile electronics. These advantages make batteries one of the most attractive devices for scientists worldwide. Solid-state batteries differ from traditional lithium-ion batteries in terms of materials, cell design, system architecture, supply chain, manufacturing procedures, and recycling techniques. Solid polymer electrolytes are an exciting option for lithium-ion batteries because of their remarkable range of characteristics. These efficiently inhibit the production of lithium dendrites and have good mechanical strength, outstanding thermal stability, and attractive electrochemical properties [1,2]. A few solid-state batteries have effectively entered the commercial market after years of intensive development, and many more are in various phases of development [3,4].

Traditionally, solid polymer electrolytes are formulated by dissolving a lithium salt in a polyethylene oxide (PEO) polymer matrix, occasionally augmented with plasticizers [5–14]. However, conventional polymer electrolytes based on PEO exhibit high crystallinity at room temperature, resulting in ionic conductivities ranging from 10^{-6} to 10^{-8} S cm⁻¹, which are levels unsuitable for solid-state batteries. Ionic-liquid-based solid electrolytes, comprising a polymer host matrix, lithium salts, and ionic liquid, offer a compelling alternative. These electrolytes boast high ionic conductivity, robust electrode–electrolyte interfaces akin to liquid electrolytes, impressive mechanical strength, flexibility, wide electrochemical windows, and thermal and chemical stability [12,15–20].

Enhancing ionic mobility and backbone flexibility in these electrolytes requires suppressing the crystalline phase [12,21]. Meghani et al. synthesized quasi-solid polymer electrolytes and found a dependence of ionic conductivity and concentration of ionic liquids in polymer electrolytes. Notably, bulk resistance tends to diminish with more significant percentages of ionic liquids beyond 10 [4]. However, though liquid plasticizers significantly increase conductivity, they frequently decrease the mechanical integrity of polymer electrolytes [4]. Typically, investigations into lithium-ion electrolyte materials occur in lithium half-cell configurations, wherein a lithium metal electrode serves as both the counter and reference electrode [7,19,22–24].

This study introduces a novel hybrid polymer electrolyte based on PEO-LiTFSI-EMIMTFSI with incorporated silica synthesized via sol–gel. This one-pot synthesis represents an alternative pathway for crafting solid polymer electrolytes tailored for solid-state batteries. This study deciphers the influence of imidazolium-based ionic liquids and incorporated silica on a salt-doped polymer electrolyte and the electrochemical stability of half-cell battery performance. Mechanically robust samples are assembled in half-cells, incorporating cathodes such as LiFePO₄ (LFP), LiNi_{0.8}Co_{0.1}Mn_{0.1}O₂ (NMC(811)), and LiCoO₂ (LCO), along with Li foil. This assembly aims to showcase the viability of these hybrid electrolytes for use in all solid-state Li-polymer batteries. The comprehensive exploration of these novel electrolytes and their performance characteristics contributes valuable insights to the ongoing advancement of solid-state battery technology.

2. Materials and Methods

2.1. Materials

The polymer poly(ethylene oxide) (PEO, $M_v = 2,000,000$ g/mol), ionic liquid 1-ethyl-3-methyl-imidazolium bis(trifluoromethylsulfonyl)imide ([EMIMTFSI], $\geq 98\%$), bis(trifluoromethane)sulfonimide lithium salt (LiTFSI, $\geq 99.95\%$), N-methyl-2-pyrrolidone (NMP, $\geq 99.5\%$), LiNi_{0.8}Co_{0.1}Mn_{0.1}O₂ (NMC(811), $\geq 99.9\%$), LiCoO₂ (LCO, $\geq 99.8\%$), LiFePO₄ (LFP, $\geq 99.9\%$), polyvinylidene fluoride (PVDF, $M_v = 40,000$ g/mol), tetraethylortosilicate (TEOS, $\geq 99\%$), and (3-glycidyloxypropyl)trimethoxysilane (GLYMO, $\geq 98\%$) were used as received from Sigma-Aldrich. All these chemicals were kept and handled inside an argon-gas-filled glove box (H_2O and $O_2 < 0.5$ ppm). Methanol (analytical grade, $H_2O < 0.02$) was used as received without further purification.

2.2. Preparation of Hybrid Polymer Electrolyte with Inorganic Filler (HPEf)

The polymer electrolytes were prepared by dissolving PEO in methanol under 50 °C, dissolving lithium salt in ionic liquid, and mixing. At the same time, the silica network part of the hybrid electrolyte was prepared using the sol–gel method: TEOS was mixed with GLYMO and hydrolyzed with 0.3 M HCl. The resulting solution was added to the PEO-LiTFSI-EMIMTFSI solution and mixed. The hybrid polymer electrolyte films (HPEf) with silica network were prepared by casting the solutions into Teflon Petri dishes (Figure 1). The obtained HPEf films were dried under room temperature for 12 h, further under high vacuum conditions for 24 h (60 °C, 2 mbar), and stored subsequently in the glove box to avoid artifacts due to humidity.

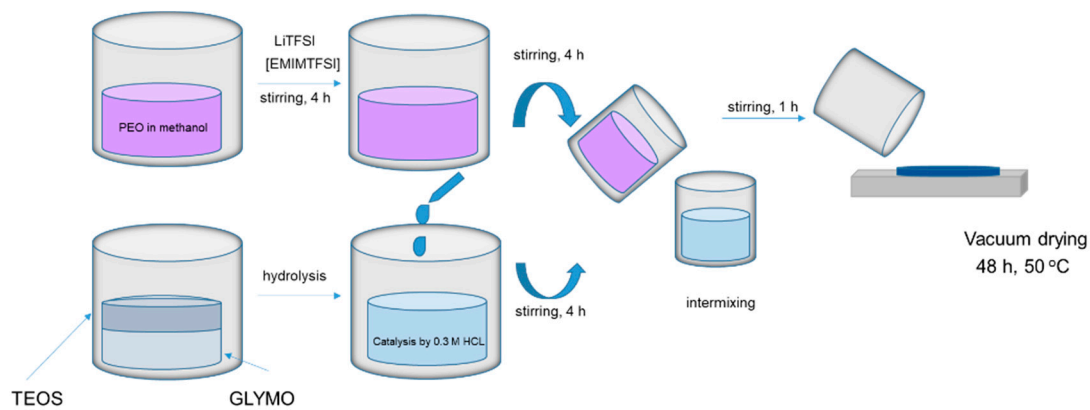


Figure 1. The preparation process of hybrid polymer electrolyte with silica network.

2.3. Preparation of Cathode Materials and Coin Half-Cell Assembling

The preparation procedure of the cathodes for the coin half-cell assembly was the following: the active powder was dispersed in a solution of polyvinylidene fluoride (PVDF) binder in N-methyl-2-pyrrolidone (NMP). The weight ratio of active powder to binder was 80:20. The homogenous slurry of the above mixtures was spread onto aluminum foil using the doctor blade technique. The solvent was evaporated at 80 °C in a drying oven for four h; then, the electrode sheet was further dried under vacuum at 120 °C for 24 h.

The CR2032 cell (Li/HPEf/NMC(811), Li/HPEf/LCO, and Li/HPEf/LFP) was assembled using lithium chips, polymer electrolyte film, and a cathode composite electrode sheet. The specific capacity of the cell is calculated according to the cathode materials. After assembly, the cells were placed inside a thermostatic chamber (Binder) set to 55 °C for 4 h before the test.

2.4. Methods

The FTIR spectra of composite electrolytes were recorded by FTIR spectrometer (Nicolet iS5, ThermoFisher, Waltham, MA, USA) from 4000 to 600 cm^{-1} . Differential scanning calorimetry (DSC) of polymer electrolyte of PEO and PEO-LiTFSI-EMIMTFSI-silica was performed using a Mettler DSC1 system in the temperature range -100 to 100 °C under a N_2 gas environment with a heating rate of 10 °C. min^{-1} .

Electrochemical and thermal stability performances of PEO-LiTFSI-EMIMTFSI-silica composite polymer electrolyte were investigated by cycling voltammetry (CV) and electrochemical impedance spectroscopy (EIS). The battery test workstation measures ionic conductivity and Li^+ ion transference number of polymer electrolytes. The electrochemical impedance spectroscopy (EIS) and CV were performed in an electrochemical workstation BT (Biologic) at 55 °C. The frequency range of EIS was 100 kHz–0.1 Hz. The galvanostatic charge–discharge measurements at 0.1 C were carried out for the half-cell assembly in the potential range of 3.0–4.2 V (vs. Li/Li^+) for NMC(811), 2.5–4.2 V (vs. Li/Li^+) for LCO, and 2.8–3.8 V and 2.5–4.3 V (vs. Li/Li^+) for LFP at 55 °C. The CV curves were obtained at a rate of 0.1 mV s^{-1} in a voltage range indicated earlier; the scan rate was chosen according to the literature [17,25]. The performance of the cells was evaluated using a battery tester in a temperature-controlled box.

3. Results

3.1. Characterization of Hybrid Polymer Electrolyte (HPEf)

3.1.1. Physico-Chemical Characterizations and Preparation of Hybrid Polymer Electrolyte (HPEf)

The synthesis of the hybrid electrolyte, incorporating PEO, LiTFSI, EMIMTFSI, and silica, involved harnessing these components' synergistic effects. Firstly, PEO was stirred to dissolve in methanol, forming a solution that served as the polymer matrix for the solid polymer electrolytes. Simultaneously, LiTFSI was dissolved in an ionic liquid, creating

a solution. Then, it was added to the PEO solution. The amalgamation was then stirred thoroughly. At the same time, the silica network, a crucial element of the hybrid electrolyte, underwent preparation using the sol-gel method. Tetraethyl orthosilicate (TEOS) was combined with (3-glycidyloxypropyl)trimethoxysilane (GLYMO) and subjected to hydrolysis with 0.3 M HCl. This process was essential for forming a well-defined silica network within the hybrid electrolyte structure.

The following step involved fabricating HPEf by casting the combined solutions into Teflon Petri dishes, as outlined in the synthesis scheme presented in Figure 1. These films underwent a carefully controlled drying process, initially at room temperature for 12 h, followed by a more extended drying period under high-vacuum conditions at 50 °C for 24 h to obtain the films. The films were then stored in a glove box to maintain their structural integrity and prevent any undesired absorption from humidity exposure. The inclusion of TFSI⁻ in the electrolyte formulation played a pivotal role in reducing the crystallinity of the PEO matrix, imparting a plasticizing effect. Additionally, TFSI⁻ enhanced the dissociation and solubility of LiTFSI within the PEO matrix due to its highly delocalized charge distribution, contributing to excellent thermal, chemical, and electrochemical stability.

Due to its slow reaction rate, the choice of TEOS for the silica network was complemented by adding GLYMO, facilitating the formation of a robust silica network. Incorporated into the polymer matrix, silica functioned as an inert filler, strategically reducing crystallinity, enhancing the amorphous regions of the PEO matrix, and ultimately promoting higher ionic conductivity. Further confirmation of the intricate interactions between silica, polymer salt, and EMIMTFSI was achieved through FTIR studies, as illustrated in Figure 2.

Compared to pure PEO, the shifting of vibrational bands in the hybrid electrolyte provided insights into the dynamic molecular interactions and the successful incorporation of each component. Peaks attributed to TFSI⁻ anion and EMIM⁺ cation vibrations and those associated with glycidyloxypropyl units offered a comprehensive understanding of the molecular landscape within the hybrid electrolyte structure. These meticulous synthesis and characterization steps lay the foundation for exploring the multifaceted properties and performance of the developed hybrid electrolyte in the context of solid-state batteries. The vibrational bands were obtained at 843, 948, 1061, 1110, 1344, 1466, and 2884 cm⁻¹ in pure PEO and were found in a hybrid electrolyte with an electrolyte solution to shift to 838, 946, 1056, 1120, 1350, and 1468 cm⁻¹. In the case of PEO-LiTFSI-EMIMTFSI, the firm peaks attributed to TFSI⁻ anion vibration (salt and IL contain the same anion) were obtained at 616, 739, 788, 1056, 1181, and 1197 cm⁻¹, and the peaks attributed to EMIM⁺ cation vibration were obtained at 650 and 1160 cm⁻¹. The vibrational bands at 2937 cm⁻¹ are attributed to the CH stretching vibrations on glycidyloxypropyl units present in GLYMO.

The appearance of new peaks at 1200 cm⁻¹ attributed to C–O–C bond formation as a result of the interaction between the C–OH groups of TEOS and the epoxy group of GLYMO under acidic conditions, as well as the shifting of PEO peaks, indicates an interaction between inorganic and organic phases of the materials. Three bands related to TFSI⁻ anions are presented in Figure S1. The bands located at 739 and 761 cm⁻¹ correspond to S–N–S stretching and CF₃ bending modes; the band at 789 cm⁻¹ is related to the combined vibration of C–S and S–N stretching [26].

3.1.2. Thermal Characterization of Hybrid Polymer Electrolyte HPEf

DSC was used to examine the phase transition behavior of hybrid electrolytes, which included different ratios of silica and pure PEO, as shown in Figure 3. A critical finding of this work is that inhibiting the crystalline phase can increase ionic mobility and backbone flexibility. Table 1 offers a thorough synopsis of the measurement data. A crystalline melting transition is seen in pure PEO, with a peak melting temperature (T_m) of 64 °C. Interestingly, the T_m values shift to 56 and 59 °C upon adding in situ scattered silica at concentrations of 5 and 10 weight percent. This occurrence suggests that the crystalline phase has been suppressed or modified, leading to changed thermal properties.

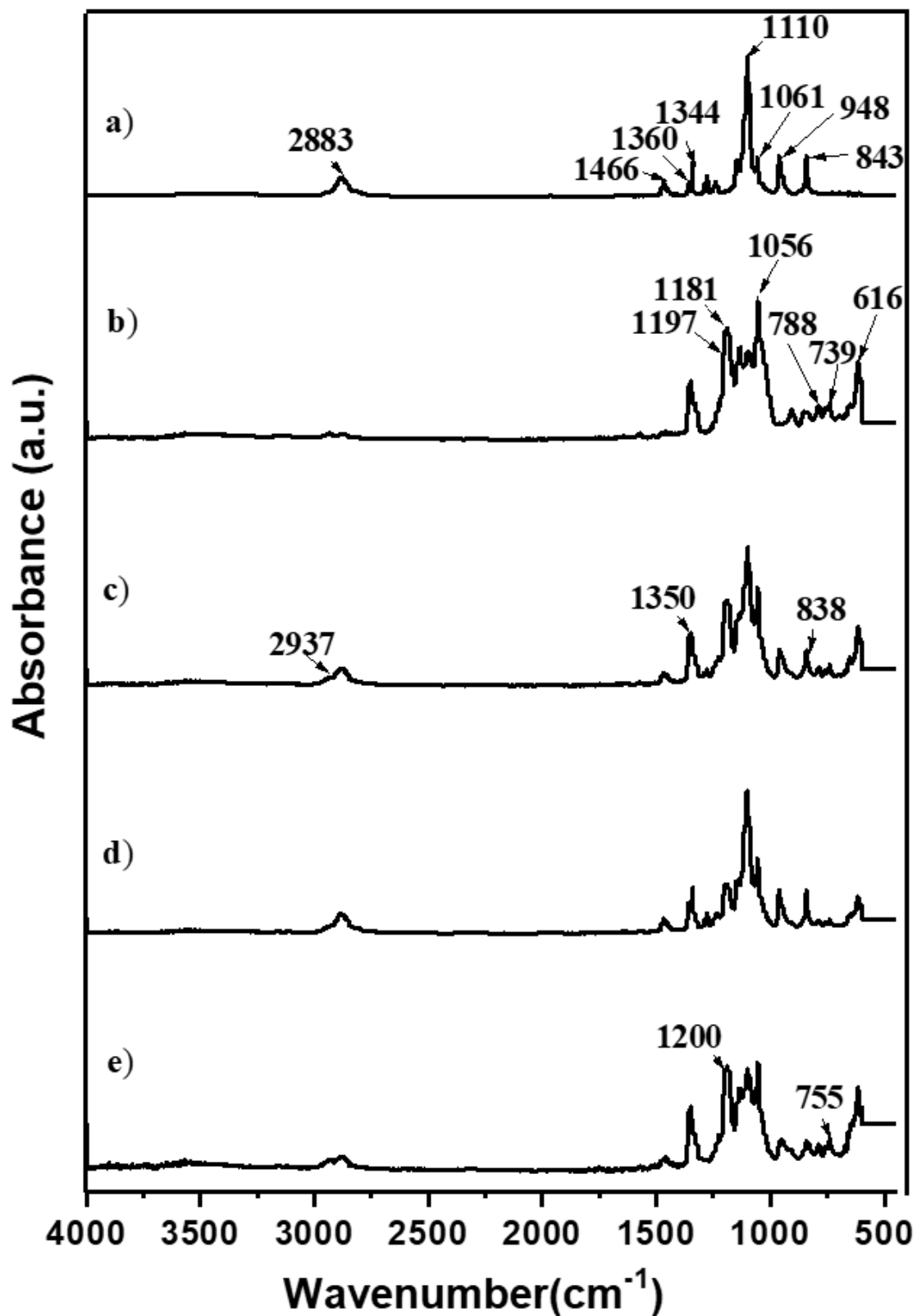


Figure 2. FTIR spectra ($4000\text{--}450\text{ cm}^{-1}$) of pure PEO (a) and hybrid polymer electrolyte *HPEf0* (b) and hybrid polymer electrolyte with silica network: (c) *HPEf25*, (d) *HPEf20*, and (e) *HPEf15*.

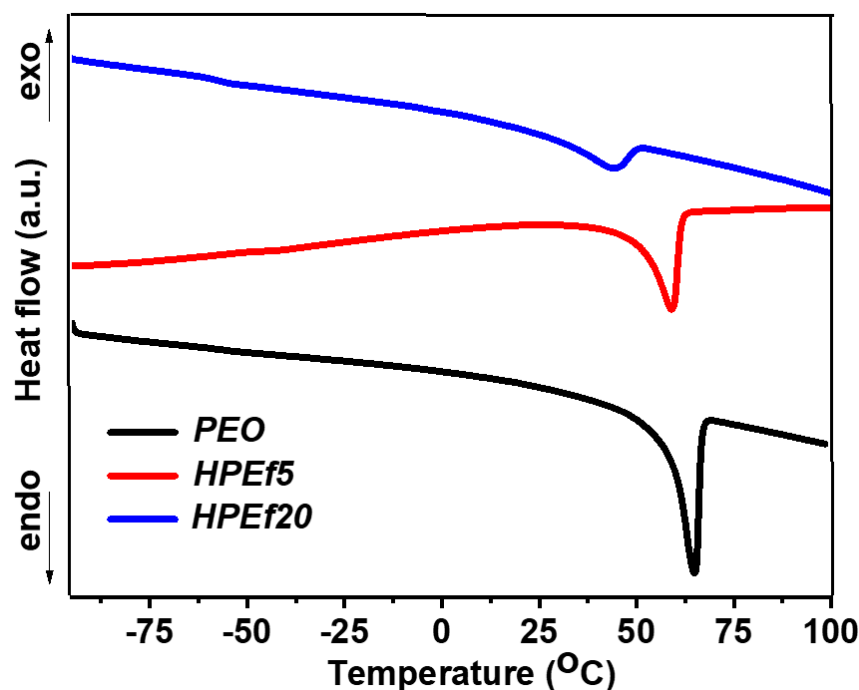


Figure 3. DSC curves of hybrid polymer electrolytes with x wt% of silica network (HPEf): $x = 20\%$ (HPEf20), $x = 5\%$ (HPEf5) and pure PEO.

Table 1. Composition of hybrid polymer electrolyte with x wt% of silica network (HPEf) and its value of glass transition temperature and melting temperature.

Composition of Hybrid Polymer Electrolyte with Inorganic Silica Network HPEf, (wt. %)							
	PEO	LiTFSI	EMIMTFSI	InorganicSilica Network	T_m (°C)	T_g (°C)	T_g^* (°C)
PEO	100	0	0	0	64	−53	
HPEf5	70	10	15	5	56	−46	−50
HPEf10	65	10	15	10	59	−49	−57
HPEf15	60	10	15	15	41	−52	−56
HPEf20	55	10	15	20	43	−54	

Furthermore, T_m values move more significantly, reaching 41 and 43 °C, for samples with the largest weight percentage of silica forming a network. This change is because eutectic mixtures, produced when PEO interacts with in situ scattered silica, give rise to a new crystalline phase.

When polyethylene oxide (PEO) is introduced into an electrolyte solution containing LiTFSI, the glass transition temperature (T_g) increases due to the interaction between ether oxygen and Li^+ ions. Throughout the study, the presence of two distinct glass transition temperatures (T_g and T_g^* , as shown in Figure S2) indicates the existence of separate microphases for PEO, ionic liquid (IL), and in situ dispersed silica. This complex behavior sheds light on the intricate interplay between silica inclusion and PEO crystallinity, suggesting the presence of two distinct phases within the hybrid electrolyte [27–29]. The lower T_g value is attributed to the interaction between PEO and EMIMTFSI, falling between the T_g values of pure PEO (−53 °C) and pure EMIMTFSI (−98 °C) [27,30]. The results offer important information about modifying hybrid electrolyte characteristics for improved performance in energy storage applications.

3.1.3. Transport Properties of Hybrid Polymer Electrolytes

The determination of ionic conductivity was executed precisely through the complex impedance method to understand the electrochemical characteristics of the hybrid polymer electrolytes. Notably, all coin cells underwent assembly within an inert Ar-filled glovebox to eliminate the influence of moisture and oxygen, thus ensuring the accuracy of subsequent measurements. The hybrid electrolytes were inserted between stainless steel blocking electrodes, demonstrating promising mechanical resilience. A controlled AC amplitude of 10 mV was applied across the cell, encompassing a broad spectrum ranging from 100 kHz to 0.1 Hz. Figure 4 shows the typical Nyquist plot recorded at an elevated temperature of 70 °C. The plot serves as a visual representation of the complex impedance, revealing distinct features that aid in interpreting the electrochemical behavior of the hybrid polymer electrolyte system. From this intricate plot, the bulk resistance, a critical parameter in understanding the overall conductivity, was accurately estimated.

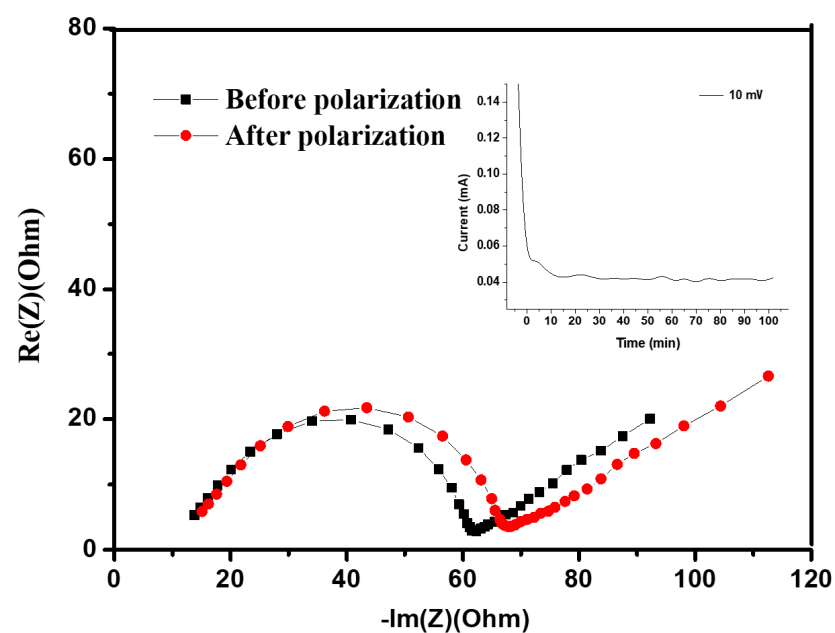


Figure 4. Impedance spectra and the time-dependence response of DC polarization for hybrid polymer electrolyte with silica network (*HPEf15*) were obtained on the symmetric cell at 70 °C, being polarized with a potential of 10 mV.

Before measurements, the preparation process was conducted for the sandwiched cell. The cell was subjected to a controlled heating regimen, reaching 60 °C for 2 h to facilitate optimal contact between components. Subsequently, the cell was allowed to equilibrate at room temperature for 24 h, ensuring stable conditions for accurate measurements. From the EIS spectrum, the bulk resistance (R_b) of the composite was obtained, and ionic conductivity was calculated based on equation $\sigma = L/(R_b S)$, where σ is the ionic conductivity, L is the thickness of the composite, and S is the contact area between the stainless steel and composite materials. Figure 5 shows the temperature-dependent ionic conductivity for the hybrid polymer electrolyte *HPEf*. The slight curvature observed in the Arrhenius plots follows the Vogel–Tamman–Fulcher model.

The lithium transference number measurements were carried out at 55 °C by combining AC impedance and DC polarization measurements using a symmetric Li/*HPEf*/Li cell. The value t^+ is calculated by the Bruce–Vincent method:

$$t^+ = \frac{I_s(\Delta V - I_0 R_{i0})}{I_0(\Delta V - I_s R_{is})}$$

where ΔV is a small d.c. bias applied to polarize the sample, and I_0 is an initial current value upon polarization with d.c. bias. I_s is a current reached in the steady state for the sample polarized with the d.c. bias, and R_{i0} and R_{is} are the resistance of solid-state electrolytes. The Li transport number of hybrid electrolytes has been estimated in Table 2.

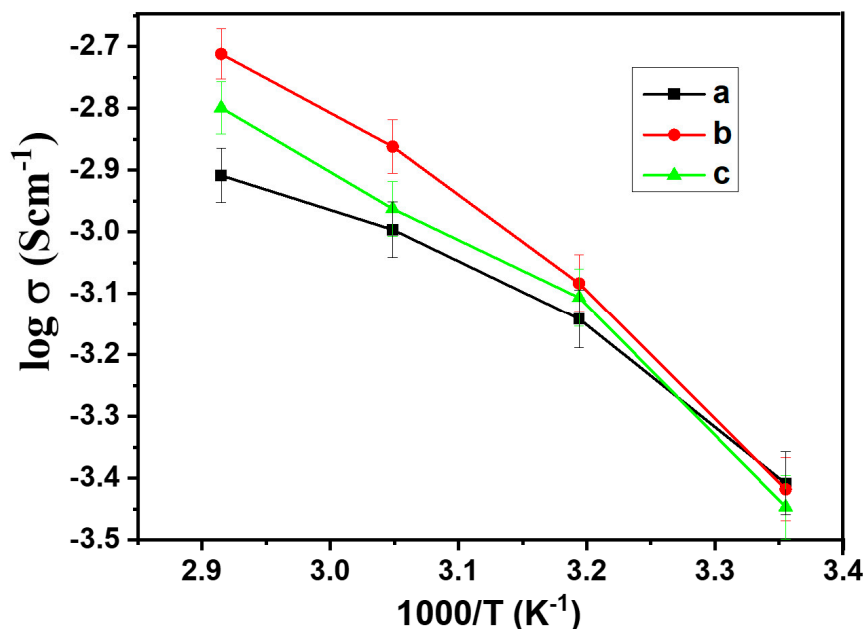


Figure 5. Arrhenius plots of ionic conductivity of hybrid polymer electrolyte, hybrid polymer electrolytes with x wt% of silica network (HPEf): (a) $x = 20\%$ (HPEf20), (b) $x = 15\%$ (HPEf15), (c) $x = 10\%$ (HPEf10). The temperature range was from 25 to 70 °C.

Table 2. Composition of hybrid polymer electrolyte with x wt% of silica network (HPEf) and its conductivity and lithium transference number at 55 °C.

Composition of Hybrid Polymer Electrolyte with Inorganic Silica Network HPEf, (wt. %)						
	PEO	LiTFSI	EMIMTFSI	InorganicSilica Network	σ (mS/cm)	t_{Li+}
HPEf20	55	10	15	20	0.101	0.284
HPEf15	60	10	15	15	0.137	0.246
HPEf10	65	10	15	10	0.109	0.235

The non-linearity of conductivity with an increase in HPEf content can be explained using polymer chain dynamics. The silica network content increases the amorphous phase in the hybrid electrolyte, which promotes the segmental motion of polymer chains (visible in the T_g value, where it gets low); this increase in segmental motion gives an increase in the ionic conductivity of the electrolyte, but when the silica network content is more than 15%, the T_g value increases slightly and lower conductivity is observed due to the restricted segmental motion of the polymer chain. Total conductivity also depends on the concentration of free mobile charge carriers [31,32].

3.2. Half-Cell Electrochemical Performance of HPE

3.2.1. Electrochemical Performance of LFP, LCO, and NMC(811) Half-Cells

Galvanostatic charge/discharge tests in half-cell configuration were carried out with LFP, LCO, and NMC(811) as cathode materials, lithium metal as the anode, and hybrid polymer electrolyte HPEf as the electrolyte and separator. The electrochemical stability was studied by cyclic voltammetry. Figure 6 shows voltammograms obtained by CV studies

at 55 °C of the prepared hybrid electrolyte. As shown in Figure 7c, the cell exhibited a potential plateau of 3.33 and 3.49 V, representing the discharge/charge potential plateau of LiFePO₄ at 0.1 C, respectively. The initial discharge capacity was 139 mAh g⁻¹, which is 81.8% of the theoretical capacity (170 mAh g⁻¹). The potential window for nmc811 was chosen for safety reasons [25] to prevent dissolution, and the observed initial discharge capacity was 143 mAh g⁻¹.

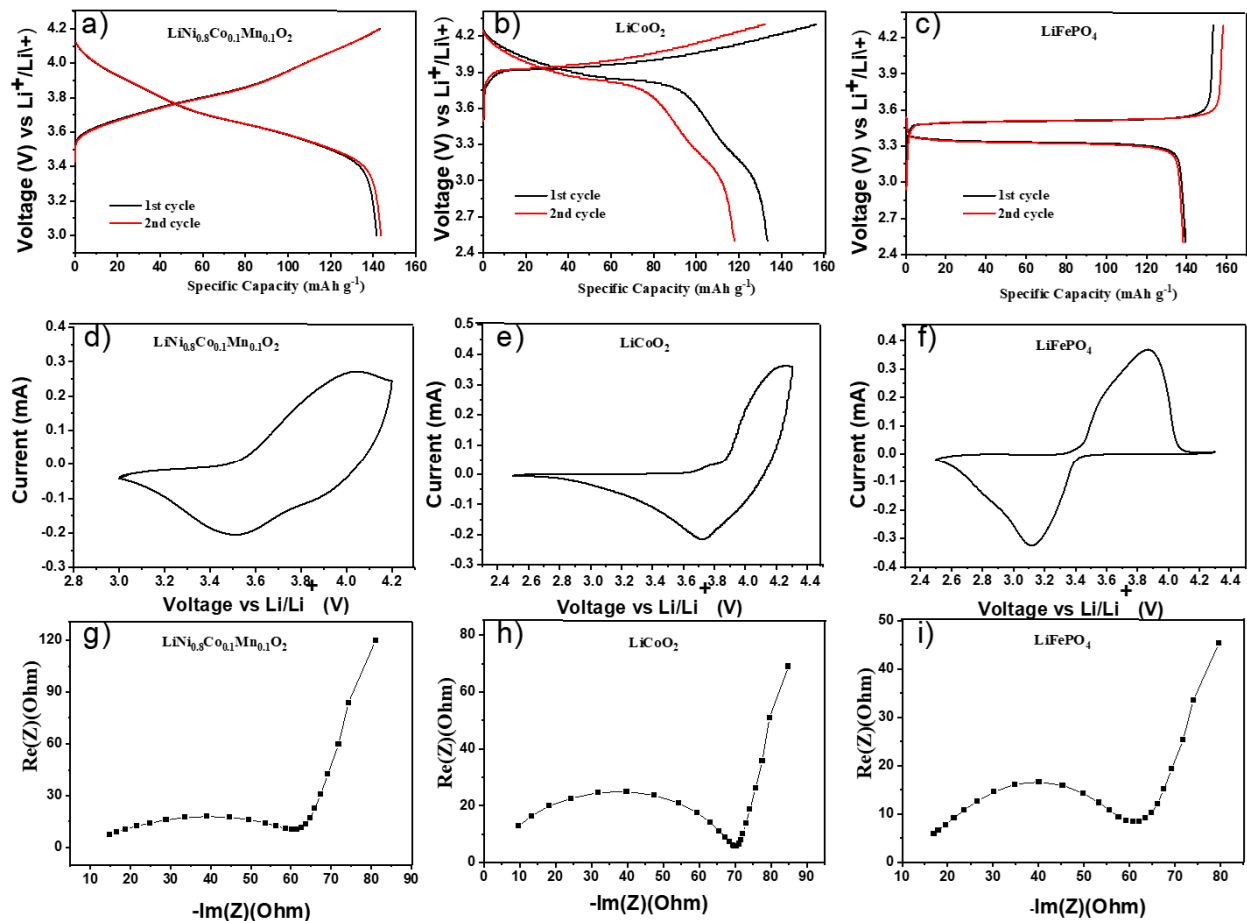


Figure 6. Electrochemical properties of hybrid polymer electrolytes with silica network in half-cells; initial CD profiles at 0.1C, CV curves at 0.1 mV/s, and EIS plots at 55 °C of LiNi_{0.8}Co_{0.1}Mn_{0.1}O₂/HPEf15/Li (a,d,g), LiCoO₂/HPEf15/Li (b,e,h), and LiFePO₄/HPEf15/Li (c,f,i) cells.

Half-cell samples of hybrid electrolytes observed differ in initial EIS with different cathode materials (Figure S3). Further investigation observed that half of the cells with LCO showed fairly high capacitance values of 135 mAh g⁻¹. However, it was discovered that the samples were nonstable and were removed from further consideration.

The electrochemical performance is explored (Figure 7) by assembling a hybrid polymer electrolyte with NMC(811) and LFP electrode materials in coin half-cells. The LFP and NMC(811) half-cells showed stable data after 30 cycles. As shown in Figure 7c, the cell exhibited a potential plateau of 3.34 and 3.48 V, representing the discharge/charge potential plateau of LiFePO₄ at 0.1 C, respectively. The initial discharge capacity was 134 mAh g⁻¹, 78.8% of the theoretical capacity (170 mAh g⁻¹). The figure also shows the capacity of Li/HPEf/LiFePO₄ cells.

The NMC(811)/HPEf10/Li and NMC(811)/HPEf15/Li half-cells show stable cycling performance and 93 and 85% capacity retention over 30 cycles. The LFP/HPEf10/Li and LFP/HPEf15/Li half-cells show stable cycling performance and capacity retention of 99.7% and 99% over 30 cycles, respectively. These results are comparable to other reported half-

cell LFP and NMC(811) battery performances with PEO-based hybrid electrolytes [Lyu, Balo, Tan]. With good mechanical and electrochemical performance, these electrolytes provide a potential approach for developing safer lithium-ion batteries.

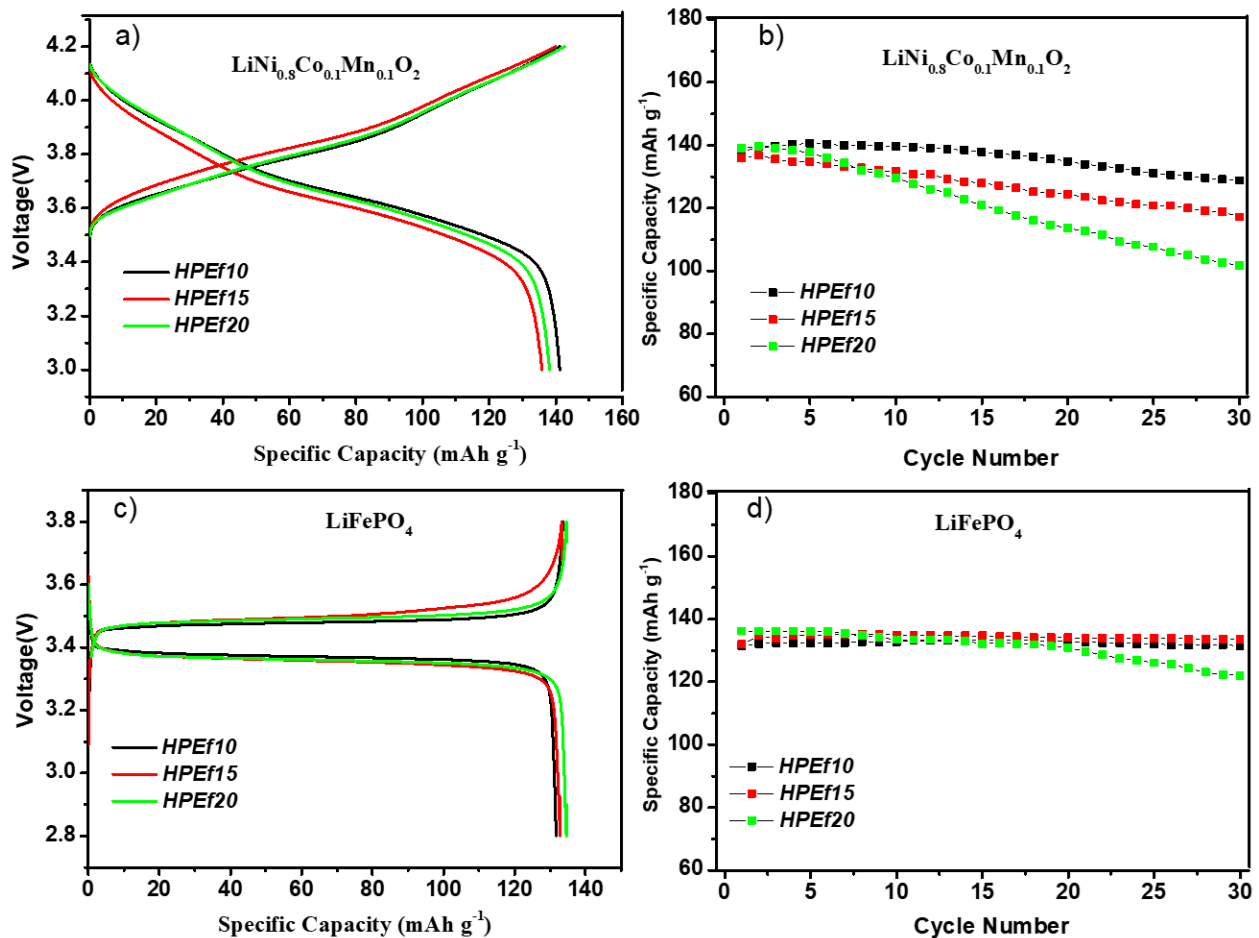


Figure 7. Initial CD profiles and CD performance of hybrid polymer electrolytes with silica network in half-cells at 0.1C at 55 °C: $\text{LiNi}_{0.8}\text{Mn}_{0.1}\text{O}_{0.1}/\text{HPEf}_x/\text{Li}$ (a,b) and $\text{LiFePO}_4/\text{HPEf}_x/\text{Li}$ cells (c,d).

3.2.2. Electrochemical Performance of LFP Half-Cell with Different Potential Window

The degradation of battery performance is a multifaceted challenge influenced by many factors, among which the electrochemical potential window and charge–discharge characteristics play crucial roles in the overall capacity decay phenomenon. Integrating hybrid electrolytes has emerged as a promising solution to address these issues. Notably, hybrid electrolytes containing 15 wt% in situ dispersed silica have demonstrated remarkable advancements in Li^+ ion conductivity, leading to superior capacitance retention in a half-cell featuring lithium iron phosphate (LFP).

Cycling experiments were conducted under varied potential windows in the LFP/HPEf15/Li samples, specifically 2.8–3.8 V and 2.5–4.3 V. As shown in Figure 8d, the results reveal exciting insights into the performance dynamics of Li/HPEf/LiFePO₄ cells. It is observed that the capacity exhibited an increase during the initial 10 cycles (under the potential window of 2.8 V to 3.8 V) and 20 cycles (within the range of 2.5 V to 4.3 V). This phenomenon can be primarily attributed to the enhanced contact and conductivity established between polyethylene oxide (PEO), the silica network, and the active material. Such improvements are particularly pronounced after repetitive Li-ion diffusion, showing the potential of these hybrid electrolytes in mitigating capacity decay issues and fostering sustained battery performance over extended cycling periods.

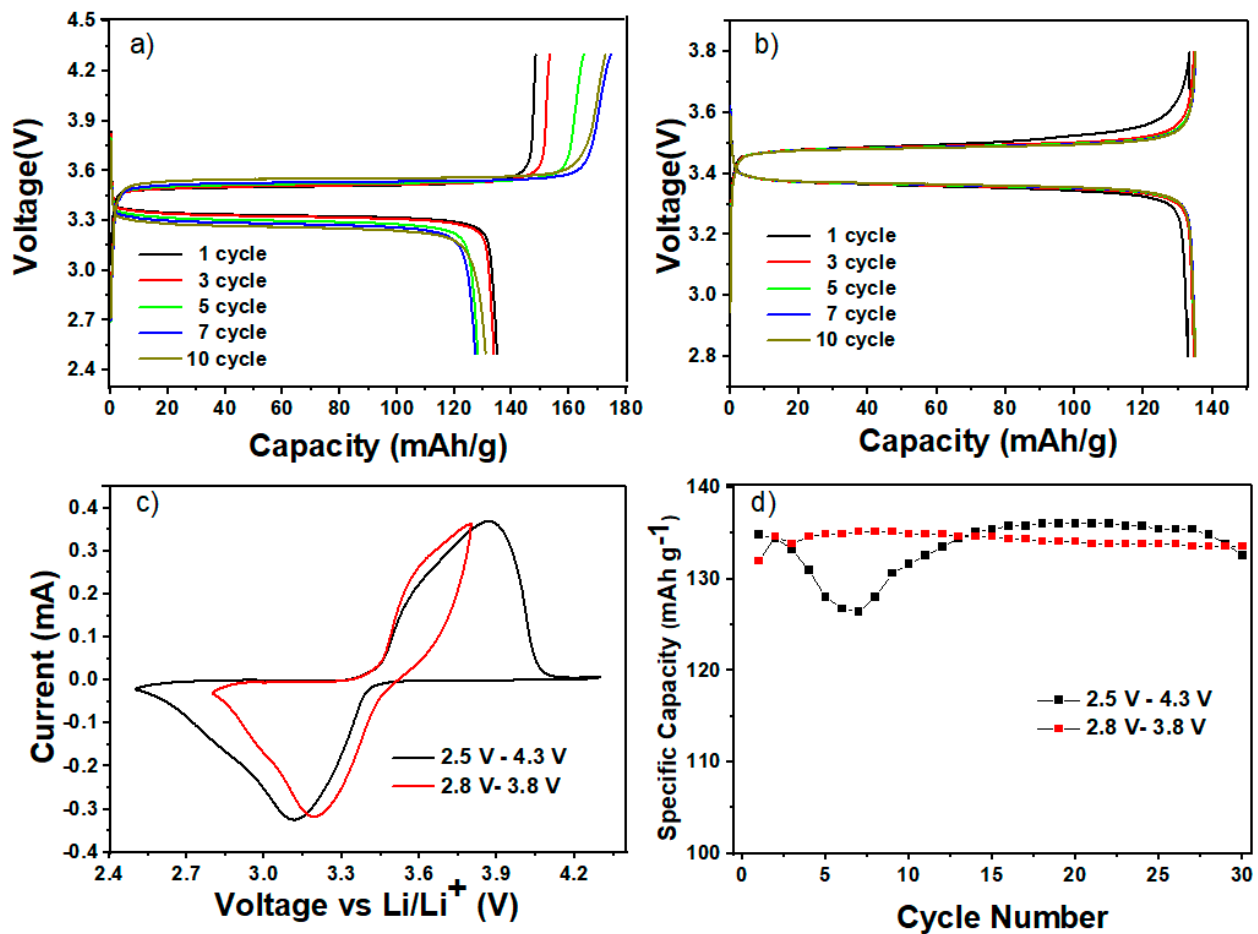


Figure 8. Electrochemical performance of hybrid polymer electrolyte in LiFePO₄/HPEf15/Li half-cell: CD profiles at 0.1 C (a,b), CV curves at 0.1 mV/s (c) and cycling performance comparison (d) between samples under the potential window of 2.5 V to 4.3 V and from 2.8 V to 3.8 V at 55 °C.

This study shows that comparable cells can have different beginning capacitances, and different amounts of capacitance retention can result from different window selections. The following stages of development for the all-solid-state battery concept require a careful balance between maintaining the ideal capacitance and obtaining exceptional cyclability. It is noteworthy that an overcharging incident at the right time might compromise the overall performance. An interesting result was obtained during testing, demonstrating a greater capacitance retention rate of 97.5% for the LFP half-cell. The maximum efficiency was reached following 100 cycles at a temperature of 55 °C. The potential window utilized to accomplish this resulted in a voltage range of 2.8 V to 3.8 V, as shown in Figure 9.

The complexity of reaching a delicate equilibrium in the performance metrics of all-solid-state batteries is clarified by this ground-breaking work, which also emphasizes how crucial temperature and potential window optimization are. The results shown here represent a significant advancement in our knowledge of the interactions between several elements affecting these batteries' performance.

Furthermore, this discovery expands its significance to the larger field of electrolyte design, going beyond the specific context of all-solid-state batteries. One important lesson is the focus on creating hybrid electrolytes with increased ionic conductivity, which might be used to improve the performance of various solid-state battery configurations. A closer look at the details of this work reveals that the pursuit of optimal electrochemical performance is closely linked to the careful design of electrolytes, opening the door to more effective and long-lasting energy storage options.

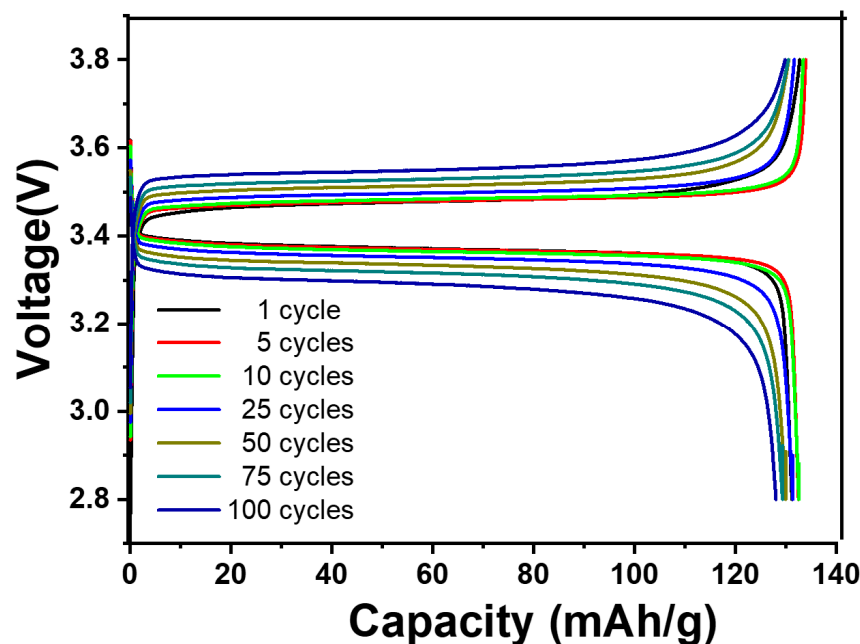


Figure 9. CD performance of LiFePO₄/HPEf15/Li at 0.1 C at 55 °C.

4. Conclusions

In this study, an array of hybrid polymer electrolytes, comprising different wt% of incorporated silica in the network, were synthesized and subjected to analysis. FTIR studies confirmed the intricate interactions among silica, the polymer salt, and EMIMTFSI, shedding light on the structural nuances of these hybrid electrolytes. The examination extended to determining transference numbers, encompassing a temperature range from 25 to 70 °C with intervals of 15 °C. Notably, the ionic conductivity of the hybrid polymer electrolytes, denoted as HPEf20, HPEf15, and HPEf10, was estimated as 0.101, 0.137, and 0.109 mS/cm, respectively, at 55 °C. Under the same conditions, the Li transport numbers for these electrolytes were found to be 0.284, 0.246, and 0.235, emphasizing their potential to facilitate efficient lithium-ion transport. Further research into the electrochemical performance of coin half-cells was conducted utilizing electrolytes in conjunction with cathode materials such as LCO, NMC(811), and LFP.

Significant attention should be directed toward the HPEf15 electrolyte, which manifested a promising initial discharge capacity of 143 mA/g for NMC(811) at 0.1 C, 134 mA/g for LCO, and 139 mA/g for LFP half-cells, all observed at 0.1 C and 55 °C. The outcomes derived from half-cells incorporating the hybrid polymer electrolytes, a Li metal anode, and a LiFePO₄ cathode were particularly noteworthy. These configurations exhibited a commendable discharge capacity of 135 mAh g⁻¹ and demonstrated exceptional capacity retention, with retention rates reaching an impressive 97.5% after 100 cycles at 0.1 C and 55 °C. We revealed that the hybrid polymer electrolytes synthesized in this study exhibit conductivity and stability window properties, rendering them promising candidates as potential electrolytes for all-solid-state batteries. The conductivity values suggest efficient ion transport within the electrolyte, while the stability windows imply robust performance under varying electrochemical conditions. These characteristics are critical for the successful operation and long-term stability of all solid-state batteries. Thus, the observed attributes of the hybrid polymer electrolytes underline their significant potential for advancing next-generation solid-state battery technology development. Our study underscores the importance of the thorough characterization and optimization of electrolyte materials for practical battery applications. Through a comprehensive evaluation of conductivity, stability, and electrochemical performance, we have demonstrated our hybrid polymer electrolytes' suitability for all-solid-state batteries. This study contributes to searching for reliable, high-performance energy storage solutions.

Supplementary Materials: The following supporting information can be downloaded at: <https://www.mdpi.com/article/10.3390/su16041683/s1>.

Author Contributions: Conceptualization, T.B.; methodology, T.B.; formal analysis, T.B.; investigation, T.B.; data curation, T.B. and Q.B.L., writing—original draft preparation, T.B. and Q.B.L.; writing—review and editing, T.B., Q.B.L. and R.K.; visualization, T.B. and Q.B.L.; supervision, T.B., Q.B.L. and R.K. All authors have read and agreed to the published version of the manuscript.

Funding: This work is mainly supported by the Ministry of Education, Youth, and Sports of the Czech Research (CZ.005).

Institutional Review Board Statement: Not applicable.

Informed Consent Statement: Not applicable.

Data Availability Statement: The data presented in this study are available on request from the corresponding author.

Conflicts of Interest: The authors declare no conflict of interest.

References

1. Angulakshmi, N.; Dhanalakshmi, R.B.; Kathiresan, M.; Zhou, Y.; Stephan, A.M. The Suppression of Lithium Dendrites by a Triazine-Based Porous Organic Polymer-Laden PEO-Based Electrolyte and Its Application for All-Solid-State Lithium Batteries. *Mater. Chem. Front.* **2020**, *4*, 933–940. [[CrossRef](#)]
2. Wang, C.; Wang, T.; Wang, L.; Hu, Z.; Cui, Z.; Li, J.; Dong, S.; Zhou, X.; Cui, G. Differentiated Lithium Salt Design for Multilayered PEO Electrolyte Enables a High-Voltage Solid-State Lithium Metal Battery. *Adv. Sci.* **2019**, *6*, 1901036. [[CrossRef](#)] [[PubMed](#)]
3. Li, J.; Li, F.; Zhang, L.; Zhang, H.; Lassi, U.; Ji, X. Recent Applications of Ionic Liquids in Quasi-Solid-State Lithium Metal Batteries. *Green Chem. Eng.* **2021**, *2*, 253–265. [[CrossRef](#)]
4. Meghni, D.; Kumar Singh, R. Ionic Liquids: Applications in Rechargeable Lithium Batteries. In *Industrial Applications of Ionic Liquids*; IntechOpen: London, UK, 2023; Volume 1, p. 13.
5. Chaurasia, S.K.; Singh, M.P.; Singh, M.K.; Kumar, P.; Saroj, A.L. Impact of Ionic Liquid Incorporation on Ionic Transport and Dielectric Properties of PEO-Lithium Salt-Based Quasi-Solid-State Electrolytes: Role of Ion-Pairing. *J. Mater. Sci. Mater. Electron.* **2022**, *33*, 1641–1656. [[CrossRef](#)]
6. Tan, X.; Wu, Y.; Tang, W.; Song, S.; Yao, J.; Wen, Z.; Lu, L.; Savilov, S.V.; Hu, N.; Molenda, J. Preparation of Nanocomposite Polymer Electrolyte via in Situ Synthesis of SiO₂ Nanoparticles in PEO. *Nanomaterials* **2020**, *10*, 157. [[CrossRef](#)]
7. Zhang, Q.; Zhang, N.; Yu, T.; Zhang, J.; Wen, B.; Zhang, L. High-Performance PEO-Based Solid-State LiCoO₂ Lithium Metal Battery Enabled by Poly(Acrylic Acid) Artificial Cathode Electrolyte Interface. *Mater. Today Energy* **2022**, *29*, 101128. [[CrossRef](#)]
8. Polu, A.R.; Rhee, H.W. Ionic Liquid Doped PEO-Based Solid Polymer Electrolytes for Lithium-Ion Polymer Batteries. *Int. J. Hydrogen Energy* **2017**, *42*, 7212–7219. [[CrossRef](#)]
9. Tripathi, A.K. Ionic Liquid-Based Solid Electrolytes (Ionogels) for Application in Rechargeable Lithium Battery. *Mater. Today Energy* **2021**, *20*, 100643. [[CrossRef](#)]
10. Chaurasia, S.K.; Chandra, A. Organic-Inorganic Hybrid Electrolytes by in-Situ Dispersion of Silica Nanospheres in Polymer Matrix. *Solid State Ionics* **2017**, *307*, 35–43. [[CrossRef](#)]
11. Yang, Z.; Fan, J.; Xu, W.; Yang, Z.; Zeng, J.; Cao, X. Solvation-Free Fabrication of PEO/LiTFSI/SiO₂ Composite Electrolyte Membranes with High Ionic Conductivity Based on a Novel Elongational Flow Field. *Ind. Eng. Chem. Res.* **2022**, *61*, 4850–4859. [[CrossRef](#)]
12. Lyu, W.; He, G.; Liu, T. PEO-LiTFSI-SiO₂-SN System Promotes the Application of Polymer Electrolytes in All-Solid-State Lithium-ion Batteries. *ChemistryOpen* **2020**, *9*, 713–718. [[CrossRef](#)]
13. Shen, X.; Li, R.; Ma, H.; Peng, L.; Huang, B.; Zhang, P.; Zhao, J. Enhancing Li⁺ Transport Kinetics of PEO-Based Polymer Electrolyte with Mesoporous Silica-Derived Fillers for Lithium-Ion Batteries. *Solid State Ionics* **2020**, *354*, 115412. [[CrossRef](#)]
14. Xi, G.; Xiao, M.; Wang, S.; Han, D.; Li, Y.; Meng, Y. Polymer-Based Solid Electrolytes: Material Selection, Design, and Application. *Adv. Funct. Mater.* **2021**, *31*, 202007598. [[CrossRef](#)]
15. Ciurduc, D.E.; Boaretto, N.; Fernández-Blázquez, J.P.; Marcilla, R. Development of High Performing Polymer Electrolytes Based on Superconcentrated Solutions. *J. Power Sources* **2021**, *506*, 230220. [[CrossRef](#)]
16. Zhu, C.; Ning, Y.; Jiang, Y.; Li, G.; Pan, Q. Double-Network Polymer Electrolytes with Ionic Liquids for Lithium Metal Batteries. *Polymers* **2022**, *14*, 3435. [[CrossRef](#)] [[PubMed](#)]
17. Herbers, L.; Küpers, V.; Winter, M.; Bieker, P. An Ionic Liquid- and PEO-Based Ternary Polymer Electrolyte for Lithium Metal Batteries: An Advanced Processing Solvent-Free Approach for Solid Electrolyte Processing. *RSC Adv.* **2023**, *13*, 17947–17958. [[CrossRef](#)] [[PubMed](#)]
18. Singh, V.K.; Shalu; Balo, L.; Gupta, H.; Singh, S.K.; Singh, R.K. Solid Polymer Electrolytes Based on Li⁺/Ionic Liquid for Lithium Secondary Batteries. *J. Solid State Electrochem.* **2017**, *21*, 1713–1723. [[CrossRef](#)]

19. Balo, L.; Shalu; Gupta, H.; Kumar Singh, V.; Kumar Singh, R. Flexible Gel Polymer Electrolyte Based on Ionic Liquid EMIMTFSI for Rechargeable Battery Application. *Electrochim. Acta* **2017**, *230*, 123–131. [[CrossRef](#)]
20. Ueki, T.; Watanabe, M. Macromolecules in Ionic Liquids: Progress, Challenges, and Opportunities. *Macromolecules* **2008**, *41*, 3739–3749. [[CrossRef](#)]
21. Zhao, S.; Wu, Q.; Ma, W.; Yang, L. Polyethylene Oxide-Based Composites as Solid-State Polymer Electrolytes for Lithium Metal Batteries: A Mini Review. *Front. Chem.* **2020**, *8*, 640. [[CrossRef](#)]
22. Li, Y.; Li, Y.; Zhang, L.; Tao, H.; Li, Q.; Zhang, J.; Yang, X. Lithiophilicity: The Key to Efficient Lithium Metal Anodes for Lithium Batteries. *J. Energy Chem.* **2023**, *77*, 123–136. [[CrossRef](#)]
23. Liu, M.; Zhang, S.; van Eck, E.R.H.; Wang, C.; Ganapathy, S.; Wagemaker, M. Improving Li-Ion Interfacial Transport in Hybrid Solid Electrolytes. *Nat. Nanotechnol.* **2022**, *17*, 959–967. [[CrossRef](#)]
24. Wood, K.N.; Noked, M.; Dasgupta, N.P. Lithium Metal Anodes: Toward an Improved Understanding of Coupled Morphological, Electrochemical, and Mechanical Behavior. *ACS Energy Lett.* **2017**, *2*, 664–672. [[CrossRef](#)]
25. Li, T.; Yuan, X.-Z.; Zhang, L.; Song, D.; Shi, K.; Bock, C. Degradation Mechanisms and Mitigation Strategies of Nickel-Rich NMC-Based Lithium-Ion Batteries. *Electrochem. Energy Rev.* **2020**, *3*, 43–80. [[CrossRef](#)]
26. Dhumal, N.R.; Noack, K.; Kiefer, J.; Kim, H.J. Molecular Structure and Interactions in the Ionic Liquid 1-Ethyl-3-Methylimidazolium Bis(Trifluoromethylsulfonyl)Imide. *J. Phys. Chem. A* **2014**, *118*, 2547–2557. [[CrossRef](#)] [[PubMed](#)]
27. Serra Moreno, J.; Armand, M.; Berman, M.B.; Greenbaum, S.G.; Scrosati, B.; Panero, S. Composite PEO:NaTFSI Polymer Electrolyte: Preparation, Thermal and Electrochemical Characterization. *J. Power Sources* **2014**, *248*, 695–702. [[CrossRef](#)]
28. Tokuda, H.; Tsuzuki, S.; Susan, M.A.B.H.; Hayamizu, K.; Watanabe, M. How Ionic Are Room-Temperature Ionic Liquids? An Indicator of the Physicochemical Properties. *J. Phys. Chem. B* **2006**, *110*, 19593–19600. [[CrossRef](#)] [[PubMed](#)]
29. Le Bideau, J.; Viau, L.; Vioux, A. Ionogels, Ionic Liquid Based Hybrid Materials. *Chem. Soc. Rev.* **2011**, *40*, 907–925. [[CrossRef](#)] [[PubMed](#)]
30. Yoshida, Y.; Muroi, K.; Otsuka, A.; Saito, G.; Takahashi, M.; Yoko, T. 1-Ethyl-3-Methylimidazolium Based Ionic Liquids Containing Cyano Groups: Synthesis, Characterization, and Crystal Structure. *Inorg. Chem.* **2004**, *43*, 1458–1462. [[CrossRef](#)] [[PubMed](#)]
31. Simonetti, E.; Carewska, M.; Maresca, G.; De Francesco, M.; Appetecchi, G.B. Highly Conductive, Ionic Liquid-Based Polymer Electrolytes. *J. Electrochem. Soc.* **2017**, *164*, A6213–A6219. [[CrossRef](#)]
32. Ye, Y.; Choi, J.-H.; Winey, K.I.; Elabd, Y.A. Polymerized Ionic Liquid Block and Random Copolymers: Effect of Weak Microphase Separation on Ion Transport. *Macromolecules* **2012**, *45*, 7027–7035. [[CrossRef](#)]

Disclaimer/Publisher’s Note: The statements, opinions and data contained in all publications are solely those of the individual author(s) and contributor(s) and not of MDPI and/or the editor(s). MDPI and/or the editor(s) disclaim responsibility for any injury to people or property resulting from any ideas, methods, instructions or products referred to in the content.